

# Realization of high-capacity hydrogen storage using carbon atomic chains: the role of terminations

Chun-Sheng Liu, Hui An, and Zhi Zeng\*

*Key Laboratory of Materials Physics, Institute of Solid State Physics,  
Chinese Academy of Sciences, Hefei 230031, P. R. China and  
Graduate School of the Chinese Academy of Sciences*

(Dated: October 27, 2018)

## Abstract

The capacity of carbon atomic chains with different terminations for hydrogen storage is studied using first-principles density functional theory calculations. Unlike the physisorption of  $\text{H}_2$  on the H-terminated chain, we show that two Li (Na) atoms each capping one end of the carbon chain can hold ten  $\text{H}_2$  molecules with optimal binding energies for room temperature storage. The hybridization of the Li  $2p$  states with the  $\text{H}_2$   $\sigma$  orbitals contributes to the  $\text{H}_2$  adsorption. However, the binding mechanism of the  $\text{H}_2$  molecules on Na arises only from the polarization interaction between the charged Na atom and the  $\text{H}_2$ . Moreover, additional  $\text{H}_2$  molecules can be bound to the carbon atoms at the chain ends due to the charge transfer between Li  $2s2p$  (Na  $3s$ ) and C  $2p$  states. Importantly, dimerization of these isolated metal-capped chains does not affect the hydrogen binding energy significantly. In addition, a single chain can be stabilized effectively by termination on the  $\text{C}_{60}$  clusters. With a hydrogen uptake of  $> 10$  wt % on Li-coated  $\text{C}_{60}\text{-C}_n\text{-C}_{60}$  ( $n = 5, 8$ ), the  $\text{Li}_{12}\text{C}_{60}\text{-C}_n\text{-Li}_{12}\text{C}_{60}$  complex, without reducing the number of adsorbed  $\text{H}_2$  molecules per Li, can serve as better building blocks of polymers than the  $(\text{Li}_{12}\text{C}_{60})_2$  dimer. These findings suggest a new route to design cluster-assembled storage materials based on terminated  $sp$  carbon chains.

---

\* Corresponding author; zzeng@theory.issp.ac.cn.

## I. INTRODUCTION

The development of economical hydrogen energy critically depends on finding efficient and safe media that can store hydrogen with high gravimetric and volumetric density.<sup>1</sup> The storage materials should also reversibly adsorb/desorb H<sub>2</sub> under ambient thermodynamic conditions. These criteria not only limit the choice of storage materials to those composed of light elements, but also require the hydrogen adsorption energy to lie between the physisorbed and chemisorbed states (0.1~0.2 eV)<sup>2</sup>.

Carbon nanostructures with  $sp^2$ -like bonding<sup>3-8</sup> have long been expected to be promising storage materials due to their light weights and large surface areas. However, hydrogen molecules bind weakly to pristine carbon materials via van der Waals interactions<sup>3</sup>. A new approach, coating the carbon surfaces with early transition metals (TMs), has recently been shown to improve storage performance<sup>4,5</sup>. These complexes not only enhance the interaction between hydrogen molecules and TMs through the Kubas interaction (hybridization of the  $d$  states with the H<sub>2</sub> states)<sup>9</sup>, but also meet the U.S. Department of Energy goal of obtaining a gravimetric capacity of 9 wt % by the year 2015. Unfortunately, preferable clustering of TM atoms on the carbon nanomaterial surfaces results in poor reversibility<sup>10</sup>. Hence, the adsorption energy of metal atoms to the substrate should be larger than the cohesive energy of the bulk metal. The use of alkali metals (AMs) and alkaline-earth metals such as Li<sup>11</sup> and Ca<sup>12</sup> to produce uniform coating has been proposed, as their cohesive energies are substantially smaller than those of TMs ( $\sim 4$  eV), but the binding energy of H<sub>2</sub> molecules in the Li<sub>12</sub>C<sub>60</sub> system is too small (0.075 eV/H<sub>2</sub>) for room temperature applications<sup>11</sup>.

In the search for a more feasible high-capacity storage medium, we now turn to the  $sp$ -hybridized carbon chains, which are considered as the important building blocks in nano-electronics and nano-mechanics. The reasons for choosing carbon chains in our study are the following: Due to their high reactivity, bare carbon chains can be stabilized by termination on a wide variety of atoms and groups<sup>13</sup>. Isolated  $sp$  chains terminated with hydrogen atoms, i.e., polyynes (with alternating singlet-triplet bonds) and cumulenes (with double C-C bonds), have already been synthesized in their basic forms<sup>14</sup>. In addition, chains with metal atoms connected to the ends have been generated<sup>15</sup>, and their magnetic, electronic, and transport properties have been studied extensively<sup>16,17</sup>. In particular, the hybrid  $sp+sp^2$  carbon-based systems<sup>18</sup>(with linear chains connecting  $sp^2$ -type fragments), repre-

senting typical interfaces in realistic nanostructures, exhibit exceptional physical and chemical properties. Recent experiments have realized single carbon chains bridging graphene nanoribbons<sup>19</sup>, and produced junctions between a single carbon chain and two single-wall carbon nanotubes (SWCN)<sup>20</sup>.

In this study, we conduct theoretical studies of hydrogen storage media consisting of H, AMs, and C<sub>60</sub> terminated cumulenes or polyynes. We show that hydrogen molecules prefer to be physisorbed rather than chemisorbed on the H-terminated carbon chains. Thus Li (Na) atoms capped carbon chains are chosen to improve the hydrogen storage performance. As a result, H<sub>2</sub> molecules are adsorbed not only on the Li or Na atoms, but also on the carbon chains. In addition, a linear periodic polymer, composed of Li atoms and five (eight)-atom carbon chain bridging C<sub>60</sub> fullerenes, can store up to  $\sim 10$  wt % of H<sub>2</sub> molecules with an average binding energy of 0.15 (0.14) eV/H<sub>2</sub>. Our results not only advance our understanding of H<sub>2</sub> adsorption on terminated carbon chains, but also offer a new avenue for efficient hydrogen storage.

## II. COMPUTATIONAL DETAILS

Numerical calculations were performed using spin-polarized density functional theory (DFT) with the Perdew-Wang (1991) exchange-correlation function<sup>21</sup>, as implemented in the DMol<sup>3</sup> package (Accelrys Inc.).<sup>22</sup> A double numerical atomic orbital augmented by *d*-polarization functions (DNP) was employed as the basis set. In the self-consistent field calculations, the electronic-density convergence threshold was set to  $1 \times 10^{-6}$  electron/Å<sup>3</sup>. Geometric optimization was performed with convergence thresholds of  $10^{-5}$  Ha for the energy,  $2 \times 10^{-3}$  Ha/Å for the force, and  $10^{-4}$  Å for the atomic displacements. We performed normal-mode analysis of the obtained structures to ensure that the structures optimized without any symmetry constraints were true minima of the potential-energy surface. To validate the above convergence parameters, the bond length and vibrational frequency of the C<sub>2</sub> dimer were calculated to be 1.312 Å and 1647 cm<sup>-1</sup>, respectively, which agree well with the corresponding experimental values of 1.31 Å and 1641 cm<sup>-1</sup><sup>23</sup>. The calculated bond length of the H<sub>2</sub> molecule (0.748 Å) is very close to the experimental value of 0.741 Å.

### III. RESULTS AND DISCUSSION

#### A. H<sub>2</sub> adsorption on H-terminated carbon chains

We first consider the physisorption of a hydrogen molecule on the standard cumulene (C<sub>5</sub>H<sub>4</sub>) and polyynes (C<sub>8</sub>H<sub>2</sub>). In Fig. 1, the lowest energy configuration of a H<sub>2</sub> molecule is located above C-C bond with the H-H molecular axis between parallel and perpendicular to the C-C bond. The adsorption energies of H<sub>2</sub> to C<sub>5</sub>H<sub>4</sub> and C<sub>8</sub>H<sub>2</sub> are about 0.05 eV and 0.08 eV, respectively, resulting from van der Waals interactions. We also calculated the adsorption energies of H<sub>2</sub> to C<sub>2n+1</sub>H<sub>4</sub> ( $n = 3, 4$ ) and C<sub>2n</sub>H<sub>2</sub> ( $n = 2, 3, 5$ ), and found that the physisorption energies did not vary significantly with the chain lengths.

Next, we investigate the H<sub>2</sub> dissociated chemisorption on C<sub>5</sub>H<sub>4</sub> or C<sub>8</sub>H<sub>2</sub> by optimizing the structure with two H atoms placed close to two adjacent C atoms (i.e., C1 and C2). Upon the atomic hydrogen adsorption, transformation of the *sp* hybridization of C1-C2 bond to the *sp*<sup>2</sup> hybridization results in a change of the bond lengths and angles. A significant elongation of the C1-C2 bond length in the chemisorption state indicates that this bond is weakened.

We apply the nudged elastic band (NEB) method to study the minimum-energy path (MEP)<sup>24</sup> of the hydrogen molecule dissociation on the carbon chains. The image number considered is 16 to ensure that the obtained MEP is correct. The physisorption of the hydrogen molecule is chosen as the initial state (PS) and the chemisorption of two hydrogen atoms as the final state (CS), as depicted in Fig. 1. From PS to CS, high barriers of 3.81 eV and 4.32 eV must be overcome. This indicates that the dissociation process of H<sub>2</sub> on C<sub>5</sub>H<sub>4</sub> or C<sub>8</sub>H<sub>2</sub> is very difficult in kinetics.

#### B. H<sub>2</sub> adsorption on Li (Na)-capped carbon chains

The above results have demonstrated that the interaction between pristine carbon chains and the hydrogen molecule is very weak, such storage systems may have to be operated at below ambient temperature. Now the question arises: can the storage performance of carbon chains be improved by using alternative capping elements? We then consider several kinds of short atomic chains (C<sub>n=5-10</sub>) terminated with two alkali metal atoms. Our full structural relaxations reveal that the linear Li<sub>2</sub>C<sub>n</sub> and Na<sub>2</sub>C<sub>n</sub> structures are more stable

and energetically favorable relative to the zigzag structures. Figure 2a illustrates that the average binding energies per Li (Na) atom with  $C_n$  chains show an even-odd oscillatory behavior. These binding energies are obviously much larger than those of Li (1.63/1.52 eV) and Na (1.11/1.41 eV) on graphene/fullerene<sup>25,26</sup>. In addition, the configurations of  $Li_2C_n$  and  $Na_2C_n$  complexes exhibit significant differences for odd or even values of  $n$ . For instance, when  $n = 5$ , the C-C distances, as depicted in Figs. 2b and 2d, are rather uniform. In contrast, the bond lengths (Figs. 2c and 2e) alternate for  $n = 8$ . This behavior implies that the bonding patterns of  $Li(Na)_2C_{2n+1}$  and  $Li(Na)_2C_{2n}$  are the same as those of  $C_{2n+1}$  and  $C_{2n}$ , respectively.

Note that the induced positive charge of the Li atom is smaller than that of Na, which is not compatible with the order of their binding energies (Fig. 2a). For example, each Li (Na) atom carries 0.39 (0.62)  $e$  and 0.43 (0.66)  $e$  in  $Li_2C_5$  ( $Na_2C_5$ ) and  $Li_2C_8$  ( $Na_2C_8$ ), respectively. We find that Li  $2p$  orbitals become partly filled due to the carbon chain back-donating some electrons to Li, whereas Na still has empty  $3p$  orbitals. This discrepancy means that the strong bonding between the Li atom and carbon chains is not simply ionic, distinctly different from the ionic bonding as the Na atom is attached to the chains. Figures 2f and 2g clearly show that the  $2p$  state of Li and the C  $p$  orbitals are hybridized for the binding of Li on the  $C_5$  and  $C_8$  chain. Since the  $p$ - $p$  hybridization is stronger than the  $s$ - $p$  hybridization, the binding energies of Li atoms to the carbon chains are larger than those of Na atoms in the  $Na_2C_n$  complexes. This bonding mechanism has also been observed in Li coated boron-doped graphenes<sup>27</sup>. In detail, the hybridization of the Li  $p_y$  orbital with the lowest unoccupied molecular orbitals (LUMO) of  $C_5$  gives rise to  $\pi$ -bonds (Fig. 2f), whereas the overlap between Li  $p_x$  and C  $p_x$  orbitals in  $Li_2C_8$  forms  $\sigma$ -bonds (Fig. 2g). Because the  $\pi$  bond is generally weaker than the  $\sigma$  bond, it is understandable that Li atoms bind more strongly to  $C_{2n}$  than that to  $C_{2n+1}$  (as revealed in Fig. 2a).

We now turn to the interaction between the metal-capped carbon chains and hydrogen. The results of our calculations present that one Li (Na) atom can attach 5  $H_2$  molecules in the  $Li_2C_5$  ( $Na_2C_5$ ) and  $Li_2C_8$  ( $Na_2C_8$ ) complexes, suggesting that the maximum number of adsorbed  $H_2$  molecules does not depend on the chain types. The optimized geometries for 5  $H_2$  molecules adsorbed on  $Li_2C_n$  and  $Na_2C_n$  ( $n = 5, 8$ ), as illustrated in Figs. 3a-3d, demonstrate that the H-H distances are slightly enlarged compared with the free  $H_2$  bond length (0.74 Å). All the side  $H_2$  molecules tend to tilt toward the chain so that one

of two H atoms of adsorbed H<sub>2</sub> molecules becomes relatively closer to the metal atom. To understand the binding mechanism of H<sub>2</sub> on Li- or Na-capped carbon chains, we employ the Mulliken charge analysis. In detail, charge transfer from the  $\sigma$  orbital of a side H<sub>2</sub> to the attached Li atom ( $\sim 0.08 e$ ) is four times larger than that to the Na atom ( $\sim 0.02 e$ ). Therefore the binding of H<sub>2</sub> to the Na atom arises basically from the induced polarization of the H<sub>2</sub> molecules by the Na atom. However the polarization interaction is not the only factor responsible for H<sub>2</sub> binding to Li due to the average binding energies of H<sub>2</sub> molecules (Figs. 3e and 3f) in Li<sub>2</sub>C<sub>5</sub>(H<sub>2</sub>)<sub>5</sub> (0.19 eV/H<sub>2</sub>) and Li<sub>2</sub>C<sub>8</sub>(H<sub>2</sub>)<sub>5</sub> (0.19 eV/H<sub>2</sub>) being slightly larger than those in Na<sub>2</sub>C<sub>5</sub>(H<sub>2</sub>)<sub>5</sub> (0.15 eV/H<sub>2</sub>) and Na<sub>2</sub>C<sub>8</sub>(H<sub>2</sub>)<sub>5</sub> (0.14 eV/H<sub>2</sub>). The analysis of molecular-orbital coefficients for the Li<sub>2</sub>C<sub>5</sub>(H<sub>2</sub>)<sub>5</sub> and Li<sub>2</sub>C<sub>8</sub>(H<sub>2</sub>)<sub>5</sub> complexes shows that the hybridization of the Li 2*p* and 2*s* states with the H<sub>2</sub>  $\sigma$  orbitals (see Figs. 3g and 3h) also contribute to the H<sub>2</sub> adsorption. The consequences of the orbital interactions are as well reflected in the charge variations of the Li. The effective charge of the Li atom in both Li<sub>2</sub>C<sub>5</sub> and Li<sub>2</sub>C<sub>8</sub> complexes varies from 0.32 to 0.06 *e* as the number of hydrogen molecules increases from 1 to 5. As a result, the binding energies of H<sub>2</sub> molecules to the Li atom slightly decrease with the increasing number of H<sub>2</sub> molecules (see Figs. 3e and 3f).

It is interesting to note that the H<sub>2</sub> molecules are adsorbed not only on the Li or Na atoms, but also on the carbon chains. Figure 4 shows that additional 8 H<sub>2</sub> molecules can be attached to Li<sub>2</sub>C<sub>5</sub>(H<sub>2</sub>)<sub>10</sub>, Li<sub>2</sub>C<sub>8</sub>(H<sub>2</sub>)<sub>10</sub>, Na<sub>2</sub>C<sub>5</sub>(H<sub>2</sub>)<sub>10</sub>, and Na<sub>2</sub>C<sub>8</sub>(H<sub>2</sub>)<sub>10</sub> complexes, resulting in hydrogen capacities of 32.7, 24.7, 25.4, and 20.2 wt %, respectively. The average binding energies of these 8 H<sub>2</sub> molecules to Li<sub>2</sub>C<sub>*n*</sub>(H<sub>2</sub>)<sub>10</sub> and Na<sub>2</sub>C<sub>*n*</sub>(H<sub>2</sub>)<sub>10</sub> (*n* = 5, 8) are 0.11 and 0.12 eV/H<sub>2</sub>, respectively, which lie within the required range of 0.1-0.2 eV. The essential reason for hydrogen attachment to the chain is that carbon atoms participate in the electron transfer, and thus the carbon chain differs from the pristine one. For instance, a C atom at the end of Li<sub>2</sub>C<sub>5</sub> (Na<sub>2</sub>C<sub>5</sub>) obtains the largest amount of electrons from Li (Na) and carries -0.37 *e* (-0.46 *e*). Very importantly, the charge on the carbon atoms does not vary during hydrogen molecules adsorbed on metal atoms. Then the electric field around the C atoms, generated by the substantial charge redistribution, can polarize the hydrogen molecules. This is confirmed through the plot of the deformation electron density (Fig. 4) which exhibits the localized characteristics of H-H bonds and no charge transfer between H and C atoms, different from the charge distribution of the side H<sub>2</sub> molecules bound to Li atoms. The H-H electric dipole vector should be parallel to the electric field direction, thus the H<sub>2</sub> molecules

align vertical to the chain in such electric field.

The above results are just promising for the isolated metal-capped carbon chains. We therefore put our further considerations on the cluster-assembled materials by using these metal-capped carbon chains as building blocks. The geometry optimization of  $M_2C_{n=5,8}$  ( $M = \text{Li}, \text{Na}$ ) dimers was performed by starting with several initial configurations. As shown in Fig. 5, two  $M_2C_n$  complexes have formed stable dimers through C-C bonds or M-C bonds but not M-M bonds due to the repulsion between the like charges. The  $(\text{Li}_2\text{C}_5)_2$  dimer has a binding energy of 3.75 eV which is substantially smaller than 7.70 eV corresponding to the  $(\text{Li}_2\text{C}_8)_2$  dimer due to C-C bonds formation between two  $\text{Li}_2\text{C}_8$  complexes. On the contrary, the binding energy of the  $(\text{Na}_2\text{C}_5)_2$  dimer (2.72 eV) is larger than that of the  $(\text{Na}_2\text{C}_8)_2$  dimer (1.74 eV). However the dimerization affects the number of adsorbed hydrogen molecules, as smaller charge on the metal atom reduces the polarization effect of the metal cation on the hydrogen molecules. As a result, the gravimetric densities obtained by the  $(\text{Li}_2\text{C}_5)_2$ ,  $(\text{Li}_2\text{C}_8)_2$ ,  $(\text{Na}_2\text{C}_5)_2$ , and  $(\text{Na}_2\text{C}_8)_2$  dimers are lowered to 14.0, 9.8, 13.1, and 11.3 wt %, respectively. Importantly, dimerizations do not change the binding energies of the  $\text{H}_2$  on metal atoms significantly, and therefore should not affect the desorption temperature.

### C. $\text{H}_2$ adsorption on $\text{Li}_{12}\text{C}_{60}\text{-C}_n\text{-Li}_{12}\text{C}_{60}$

From above, we have seen that the type of chain-termination turns out to influence the hydrogen adsorption performance. Here we have considered the  $sp^2$ -terminated  $C_n$  chains as potential storage media by choosing  $C_{60}$  fullerene as the end-capping candidate, because it not only mimics the inner SWNT caps<sup>20</sup> but also can hold metal atoms to attach hydrogen molecules. We find that  $C_n$  chains, regardless of  $n$  being odd or even, energetically prefer to bind the common bond of two hexagons ( $[6,6]$ ), resulting in the  $C_{60}\text{-C}_{2n+1}\text{-C}_{60}$  and  $C_{60}\text{-C}_{2n}\text{-C}_{60}$  complexes with  $D_{2d}$  and  $D_{2h}$  symmetry, respectively. As show in Figs. 6a and 6b, the bond lengths of the  $C_5$  ( $C_8$ ) chain in  $C_{60}\text{-C}_5\text{-C}_{60}$  ( $C_{60}\text{-C}_8\text{-C}_{60}$ ) imply a polyynes (cumulene) structure. The binding energy is calculated by subtracting the equilibrium total energy of the  $C_{60}\text{-C}_n\text{-C}_{60}$  complex from the sum of the total energy of isolated chain ( $C_n$ ) and of  $C_{60}$  clusters. The structure of two  $C_{60}$  clusters bridged by the  $C_5$  ( $C_8$ ) chain with a binding energy of 4.46 eV (4.94 eV) is more stable than the dumbbell-like structure of  $C_{60}$  dimers<sup>28</sup>. The stability of  $C_{60}\text{-C}_n\text{-C}_{60}$  ( $n = 5, 8$ ) has been further verified by carrying out *ab initio*

molecular dynamics simulations at 800 K with a time step of 1 fs. After running 5000 steps, the geometry is still kept although the chain is slightly distorted, suggesting that the  $C_{60}$ - $C_n$ - $C_{60}$  complexes are stable. This is confirmed by recent theoretical results that  $C_{60}$ - $C_8$ - $C_{60}$  can be stable up to a temperature of 1000 K<sup>20</sup>.

Considering the Li atoms interacting with the  $C_{60}$ - $C_n$ - $C_{60}$  ( $n = 5, 8$ ) complex, it is found that the pentagonal face of  $C_{60}$  is the preferred site. A close examination of the geometry of the  $Li_{12}C_{60}$ - $C_n$ - $Li_{12}C_{60}$  configuration, as depicted in Figs. 6c and 6d, illustrates that the 12 Li atoms adsorbed on each  $C_{60}$  cluster are divided into two sets. The Mulliken charge analysis presents that the Li  $2p$  orbitals are partly filled. Thus the hybridization between the Li  $2p$  and C  $2p$  orbitals strengthens the Li binding to  $C_{60}$ . The average binding energy per Li atom with  $C_{60}$  in  $Li_{12}C_{60}$ - $C_5$ - $Li_{12}C_{60}$  (1.74 eV) or  $Li_{12}C_{60}$ - $C_8$ - $Li_{12}C_{60}$  (1.76 eV) is larger than that in the isolated  $Li_{12}C_{60}$  (1.71 eV) and the Li bulk cohesive energy (1.63 eV experimental value). Hence the clustering of Li atoms will not occur in our models.

We now enter the next phase of our calculation, namely, to discuss the possible number of hydrogen molecules that can be bound to the  $Li_{12}C_{60}$ - $C_5$ - $Li_{12}C_{60}$  and  $Li_{12}C_{60}$ - $C_8$ - $Li_{12}C_{60}$  structures. Previous studies have suggested that 5  $H_2$  molecules can be bound to each Li atom in the isolated  $Li_{12}C_{60}$  cluster, whereas the binding energy of the fifth  $H_2$  molecule is only 0.06 eV<sup>12</sup>. Therefore we consider if each Li atom can adsorb 4  $H_2$  molecules in both  $Li_{12}C_{60}$ - $C_5$ - $Li_{12}C_{60}$  and  $Li_{12}C_{60}$ - $C_8$ - $Li_{12}C_{60}$  structures, corresponding to 10.3 and 10.1 wt % gravimetric densities, respectively. The average binding energies of 96  $H_2$  molecules with  $Li_{12}C_{60}$ - $C_5$ - $Li_{12}C_{60}$  (Fig. 7a) and  $Li_{12}C_{60}$ - $C_8$ - $Li_{12}C_{60}$  (Fig. 7a) are 0.16 eV. The equilibrium H-H bond lengths are 0.755 Å, which is comparable to that in  $Li_{12}C_{60}(H_2)_{60}$ , namely, 0.753 Å. The shortest and longest distances between the Li atom and H atoms are observed to be of the order of 2.330-2.750 Å.

As mentioned above, a single carbon chain bridging two  $Li_{12}C_{60}$  clusters does not change the number of adsorbed hydrogen molecules per Li. In contrast, a  $(Li_{12}C_{60})_2$  dimer would lower the hydrogen storing capacity because some of the Li atoms linking  $Li_{12}C_{60}$  clusters may not be able to attach hydrogen molecules<sup>12</sup>. Now readers have to ask whether the  $Li_{12}C_{60}$ - $C_n$ - $Li_{12}C_{60}$  structures can form the building blocks of a new kind of solid storage materials? To address this question, we first consider the adsorption of Li atoms on linear periodic  $C_{60}$ - $C_n$ - $C_{60}$  polymers. After full symmetry unrestricted geometry optimization,  $Li_{12}C_{60}$ - $C_n$ - $Li_{12}C_{60}$  units can maintain their structural identity. The binding energy of Li



atoms to a linear periodic  $C_{60}\text{-}C_5\text{-}C_{60}$  ( $C_{60}\text{-}C_8\text{-}C_{60}$ ) polymer is 1.80 (1.76) eV/Li, respectively, indicating that the polymerization has not affected the binding strength of Li to  $C_{60}$ . On the experimental side, one-dimensional<sup>28</sup> or two-dimensional<sup>29</sup>  $C_{60}$  polymers, the hexagonal faces interact with each other, have been synthesized by several methods. For the fabrication of  $C_{60}\text{-}C_n\text{-}C_{60}$  polymer, we propose a possible route to use the SWNT/single-carbon-chain molecular junctions<sup>20</sup> as the initial materials. Second, each Li atom in the polymer composed of  $Li_{12}C_{60}\text{-}C_5\text{-}Li_{12}C_{60}$  ( $Li_{12}C_{60}\text{-}C_8\text{-}Li_{12}C_{60}$ ), shown in Fig. 8, can hold 4  $H_2$  molecules with an average binding energy of 0.15 eV/ $H_2$  (0.14 eV/ $H_2$ ), resulting in the maximum gravimetric density of 10 wt % (9.6 wt %). This not only meets the gravimetric density target set by the U.S. Department of Energy for the year 2015, but the hydrogen binding energy is also optimal for the system operation under ambient thermodynamic conditions.

#### IV. CONCLUSIONS

In conclusion, the adsorption of  $H_2$  molecules on H, AMs, and  $C_{60}$  terminated carbon chains was studied using all-electron DFT calculations. It is energetically favorable for  $H_2$  to physisorb on the H terminated chains. However, for Li or Na atoms capping the chain ends,  $H_2$  molecules are adsorbed not only on the metal atoms but also on the carbon atoms with the required adsorption energy. Although the dimerization of  $M_2C_n$  ( $M = Li, Na$ ) lower the hydrogen uptake, the binding energy of the  $H_2$  on metal atoms is not affected significantly. Thus one may assemble these metal-capped carbon chains to synthesize efficient storage media or catalysts. Furthermore, we propose a linear periodic polymer, consisting of  $Li_{12}C_{60}\text{-}C_5\text{-}Li_{12}C_{60}$  ( $Li_{12}C_{60}\text{-}C_8\text{-}Li_{12}C_{60}$ ), can store up to  $\sim 10$  wt % of  $H_2$  molecules with an average binding energy of 0.15 (0.14) eV/ $H_2$ . We believe that current results presented here can be applied to other carbon chain bridging metal-coated  $sp^2$  materials. We also hope these results may provide a useful reference for the design of bulk hydrogen storage materials in the laboratory.

#### V. ACKNOWLEDGMENTS

This work was supported by the National Science Foundation of China under Grant no. 10774148, the special funds for the Major State Basic Research Project of China (973) under

Grant no. 2007CB925004, and the Knowledge Innovation Program of the Chinese Academy of Sciences. Part of the calculations were performed at the Center for Computational Science of CASHIPS. We thank P. Jena for useful suggestions.

---

- <sup>1</sup> Schlapbach, L; Züttel, A. *Nature (London)* **2001**, *414*, 353.
- <sup>2</sup> Bhatia, S. K.; Myers, A. L. *Langmuir* **2006**, *22*, 1688.
- <sup>3</sup> Dillon, A. C.; Jones, K. M.; Bekk Dahl, T. A.; Kiang, C. H.; Bethune, D. S.; Heben, M. J. *Nature (London)* **1997**, *386*, 377.
- <sup>4</sup> Yildirim, T.; Ciraci, S. *Phys. Rev. Lett.* **2005**, *94*, 175501.
- <sup>5</sup> Zhao, Y. F.; Kim, Y. H.; Dillon, A. C.; Heben, M. J.; Zhang, S. B. *Phys. Rev. Lett.* **2005**, *94*, 155504.
- <sup>6</sup> Lee, H.; Choi, W. I.; Ihm, J. *Phys. Rev. Lett.* **2006**, *97*, 056104.
- <sup>7</sup> Durgun, E.; Ciraci, S.; Zhou, W.; Yildirim, T. *Phys. Rev. Lett.* **2006** *97*, 226102.
- <sup>8</sup> Kim, Y. H.; Zhao, Y. F.; Williamson, A.; Heben, M. J.; Zhang, S. B. *Phys. Rev. Lett.* **2006**, *96*, 016102.
- <sup>9</sup> Kubas, G. J.; Ryan, R. R.; Swanson, B. I.; Vergamini, P. J.; Wasserman, H. J. *J. Am. Chem. Soc.* **1984**, *106*, 451.
- <sup>10</sup> Sun, Q.; Wang, Q.; Jena, P.; Kawazoe, Y. *J. Am. Chem. Soc.* **2005**, *127*, 14582.
- <sup>11</sup> Sun, Q.; Jena, P.; Wang, Q.; Marquez, M. *J. Am. Chem. Soc.* **2006**, *128*, 9741.
- <sup>12</sup> Yoon, M.; Yang, S.; Hicke, C.; Wang, E.; Geohegan, D.; Zhang, Z. *Phys. Rev. Lett.* **2008**, *100*, 206806.
- <sup>13</sup> Burnin, A; BelBruno, J. J. *J. Phys. Chem. A* **2003**, *107*, 9547 (2003).
- <sup>14</sup> Gu, X.; Kaiser, R. I.; Mebel, A. M. *Chem. Phys. Chem.* **2008**, *9*, 350.
- <sup>15</sup> Roth, G.; Fischer, H. *Organometallics* **1996**, *15*, 5766, and references therein.
- <sup>16</sup> Lang, N. D.; Avouris, Ph. *Phys. Rev. Lett.* **1998**, *81*, 3515; *Phys. Rev. Lett.* **2000**, *84*, 358.
- <sup>17</sup> Durgun, E.; Senger, R. T.; Sevincli, H.; Mehrez, H.; Ciraci, S. *Phys. Rev. B* **2006**, *74*, 235413; Dag, S.; Tongay, S.; Yildirim, T.; Durgun, E.; Senger, R. T.; Fong, C. Y.; Ciraci, S. *Phys. Rev. B* **2005**, *72*, 155444.
- <sup>18</sup> Ravagnan, L.; Manini, N.; Cinquanta, E.; Onida, G.; Sangalli, D.; Motta, C.; Devetta, M.; Bordoni, A.; Piseri, P.; Milani, P. *Phys. Rev. Lett.* **2009**, *102*, 245502; Ravagnan, L.; Siviero,

- F.; Lenardi, C.; Piseri, P.; Barborini, E.; Milani, P.; Casari, C. S.; Li Bassi, A.; Bottani, C. E. *Phys. Rev. Lett.* **2002**, *89*, 285506; Ravagnan, L.; Bongiorno, G.; Bandiera, D.; Salis, E.; Piseri, P.; Milani, P.; Lenardi, C.; Coreno, M.; de Simone, M.; Prince, K. C. *Carbon* **2006**, *44*, 1518; Bogana, M. P.; Colombo, L. *Appl. Phys. A* **2007**, *86*, 275.
- <sup>19</sup> Jin, C.; Lan, H., Peng, L., Suenage K.; Iijima, S. *Phys. Rev. Lett.* **2009**, *102*, 205501; Chuvilin, A.; Meyer, J. C.; Siller, G. A.; Kaiser, U. *New J. Phys.* **2009**, *11*, 083019.
- <sup>20</sup> Börrnert, F.; Börrnert, C.; Gorantla, S.; Liu, X.; Bachmatiuk, A.; Joswig, J. O.; Wagner, F. R.; Schäffel, F.; Warner, J. H.; Schönfelder, R.; Rellinghaus, B.; Gemming, T.; Thomas, J.; Knupfer, M.; Büchner, B.; Rümmeli, M. H. *Phys. Rev. B* **2010**, *81*, 085439.
- <sup>21</sup> Wang, Y.; Perdew, J. P. *Phys. Rev. B* **1991**, *44*, 13298; Perdew, J. P.; Wang, Y. *Phys. Rev. B* **1992**, *45*, 13244.
- <sup>22</sup> Delley, B. *J. Chem. Phys.* **1990**, *92*, 508.
- <sup>23</sup> Hutter, J.; Lüthi, H. P.; Diederich, F. *J. Am. Chem. Soc.* **1994**, *116*, 750.
- <sup>24</sup> Henkelman, G.; Jónsson, H. *J. Chem. Phys.* **2000**, *113*, 9978; Olsen, R. A.; Kroes, G. J.; Henkelman, G.; Arnaldsson, A.; Jónsson, H. *J. Chem. Phys.* **2004**, *121*, 9776.
- <sup>25</sup> Chan, K. T.; Neaton, J. B.; Cohen, M. L. *Phys. Rev. B* **2008**, *77*, 235430.
- <sup>26</sup> Chandrakumar, K. R. S.; Ghosh, S. K. *Nano lett.* **2008**, *8*, 13.
- <sup>27</sup> Liu, C. S.; Zeng, Z. *Appl. Phys. Lett.* **2010**, *96*, 123101.
- <sup>28</sup> Beu, T. A.; Onoe, J.; Hida, A. *Phys. Rev. B* **2005**, *72*, 155416.
- <sup>29</sup> Onoe, J.; Nakayama, T.; Aono, M.; Hara, T. *J. Appl. Phys.* **2004**, *96*, 443.

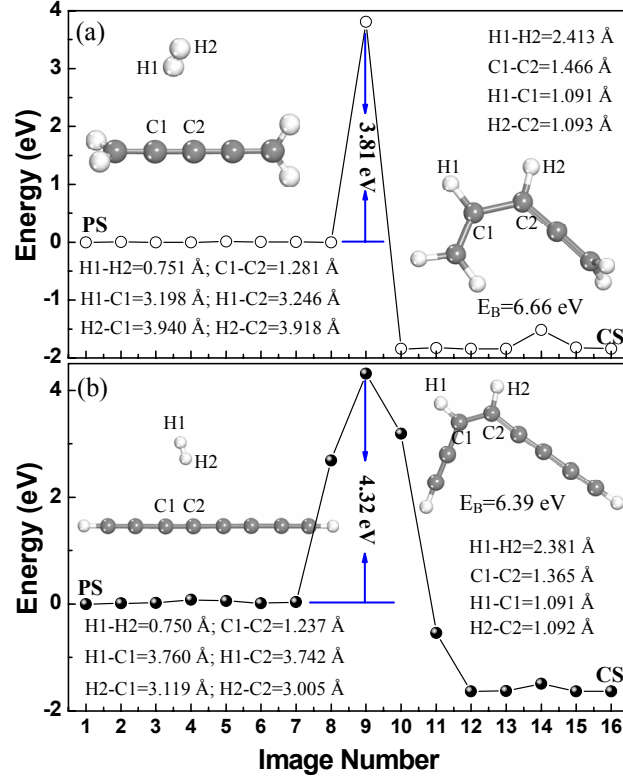


FIG. 1: The MEPs for the dissociation process of H<sub>2</sub> on the (a) C<sub>5</sub>H<sub>4</sub> and (b) C<sub>8</sub>H<sub>2</sub>. The energy of the initial structure (PS) is set as zero. The relevant bond distances and binding energy (E<sub>B</sub>) are also given.

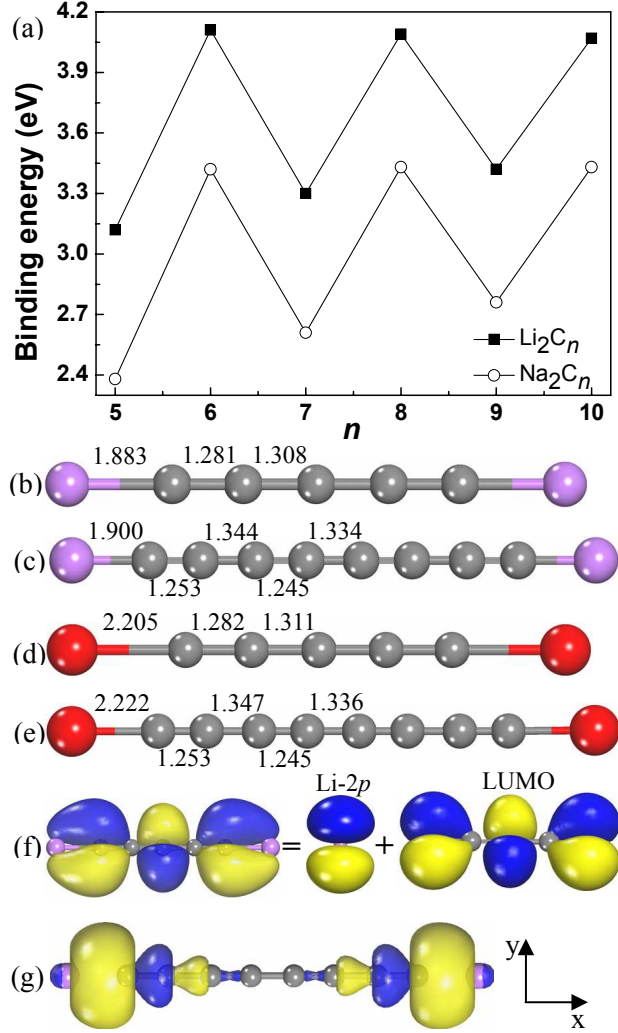


FIG. 2: (a) Average binding energies of two Li or Na atoms on  $\text{C}_n$  as a function of the number of carbon atoms. The optimized bond lengths (in Å) of (b)  $\text{Li}_2\text{C}_5$ , (c)  $\text{Li}_2\text{C}_8$ , (d)  $\text{Na}_2\text{C}_5$ , and (e)  $\text{Na}_2\text{C}_8$ . The large (red), medium (purple), and small (grey) balls represent the Na, Li, and C atoms, respectively. The panel (f) shows the  $\text{Li}_2\text{C}_5$  bonding orbital results from the hybridization of the Li  $2p$  orbital and  $\text{C}_5$  LUMO. (g) The bonding orbital for the Li atoms attached to  $\text{C}_8$ . The isovalue equals  $0.015 \text{ e}/\text{\AA}^3$ . The two colors denote  $\pm$  signs of the wave function.

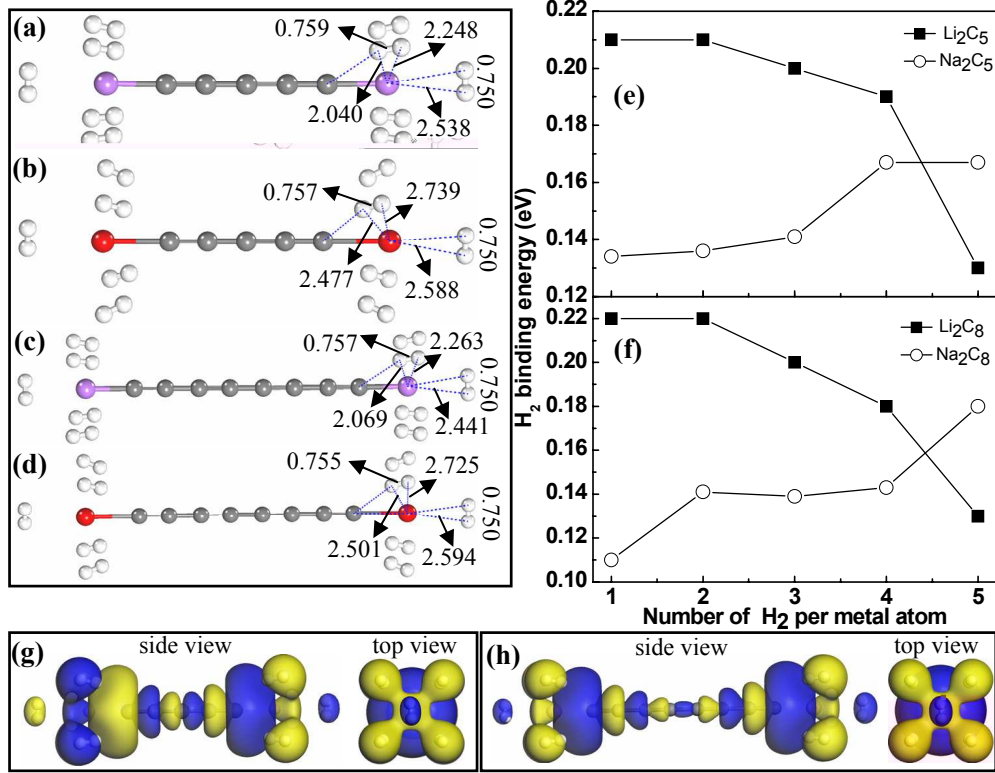


FIG. 3: Optimized configurations of H<sub>2</sub> molecules adsorbed on (a) Li<sub>2</sub>C<sub>5</sub>, (b) Na<sub>2</sub>C<sub>5</sub>, (c) Li<sub>2</sub>C<sub>8</sub>, and (d) Na<sub>2</sub>C<sub>8</sub> along with the typical bond lengths (in Å). Panels (e) and (f) show the hydrogen binding energies with successive additions of H<sub>2</sub> molecules to each metal atom in M<sub>2</sub>C<sub>n</sub> (M = Li, Na; n = 5, 8). Panels (g) and (h) show the orbitals for the side hydrogen molecules hybridized with the Li 2p orbitals in Li<sub>2</sub>C<sub>5</sub>(H<sub>2</sub>)<sub>5</sub> and Li<sub>2</sub>C<sub>8</sub>(H<sub>2</sub>)<sub>5</sub>, respectively. The isovalue equals 0.01 e/Å<sup>3</sup>.

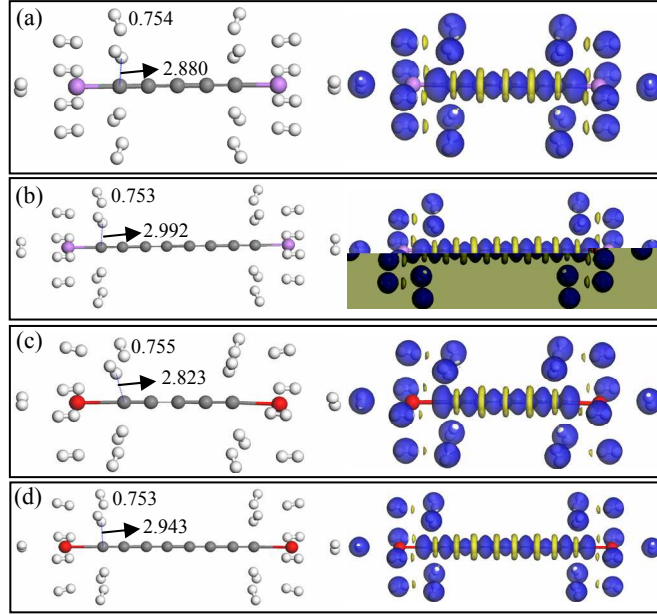


FIG. 4: Final optimized geometries of (a)  $\text{Li}_2\text{C}_5(\text{H}_2)_5$ , (b)  $\text{Li}_2\text{C}_8(\text{H}_2)_5$ , (c)  $\text{Na}_2\text{C}_5(\text{H}_2)_5$ , and (d)  $\text{Na}_2\text{C}_8(\text{H}_2)_5$  holding additional eight  $\text{H}_2$  molecules. The relevant bond distances (in  $\text{\AA}$ ) are given. The right panels (a), (b), (c), and (d) show the corresponding deformation electron densities (molecular charge densities minus atomic charge densities). The deformed density marked in blue corresponds to the region that contains excess electrons, while that marked in yellow indicates electron loss. The isovalue equals  $0.1 \text{ e}/\text{\AA}^3$ .

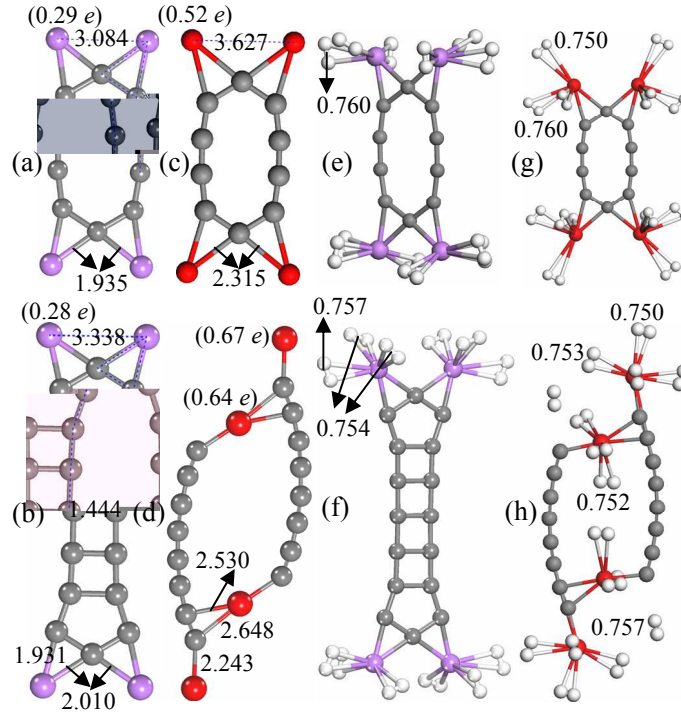


FIG. 5: Atomic configurations of dimers of (a)  $\text{Li}_2\text{C}_5$ , (b)  $\text{Li}_2\text{C}_8$ , (c)  $\text{Na}_2\text{C}_5$ , and (d)  $\text{Na}_2\text{C}_8$ . Geometries of (e)  $\text{Li}_2\text{C}_5$ , (f)  $\text{Li}_2\text{C}_8$ , (g)  $\text{Na}_2\text{C}_5$ , and (h)  $\text{Na}_2\text{C}_8$  dimers respectively holding 12, 12, 12, and 18  $\text{H}_2$  molecules. The numbers in parentheses refer to charges on metal atoms, while other numbers refer to bond lengths in Å.



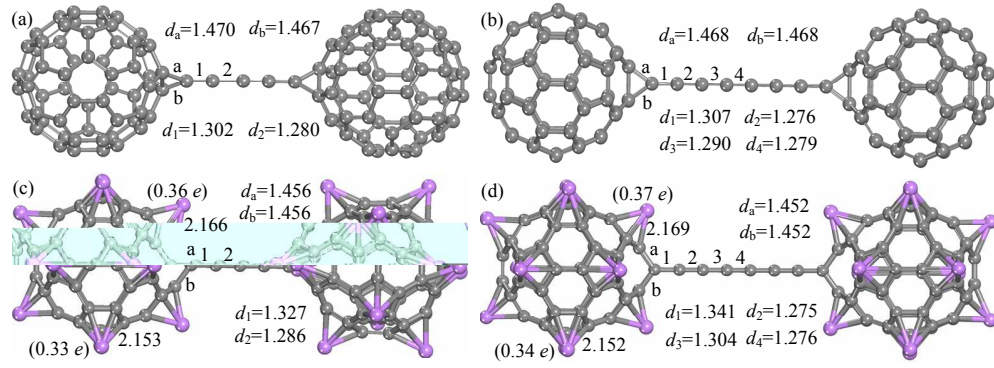


FIG. 6: Atomic configurations of (a)  $C_{60}-C_5-C_{60}$ , (b)  $C_{60}-C_8-C_{60}$ , (c)  $Li_{12}C_{60}-C_5-Li_{12}C_{60}$ , and (d)  $Li_{12}C_{60}-C_8-Li_{12}C_{60}$ . The numbers in parentheses denote charges on the Li atoms. The typical bond lengths are given in  $\text{\AA}$ .

FIG. 7: Panels (a) and (b) show the four  $H_2$  molecules adsorbed on each Li atom in  $Li_{12}C_{60}-C_5-Li_{12}C_{60}$  and  $Li_{12}C_{60}-C_8-Li_{12}C_{60}$ .

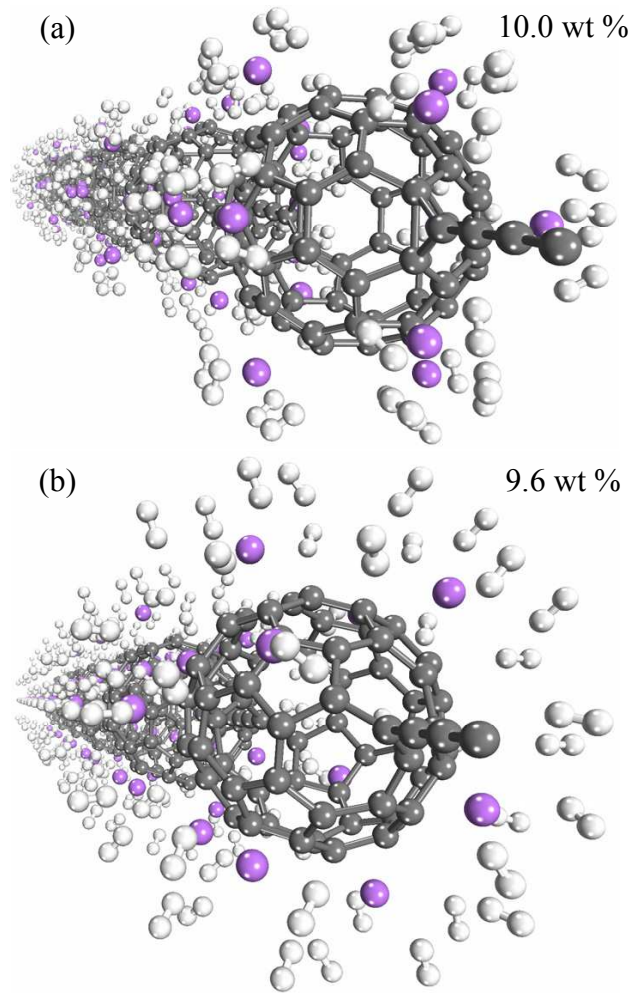


FIG. 8: Panels (a) and (b) show the  $\text{H}_2$  molecules adsorbed on the periodic polymers composed of  $\text{Li}_{12}\text{C}_{60}\text{-C}_5\text{-Li}_{12}\text{C}_{60}$  and  $\text{Li}_{12}\text{C}_{60}\text{-C}_8\text{-Li}_{12}\text{C}_{60}$ , respectively.

